8

Maximum Power Point Tracking

The output of PV cells is limited by the current, voltage, and power. In a steady state of solar irradiance and cell temperature, there is a single operating point where the output of the voltage and current results in the maximum power output. The maximum power point (MPP) is occasionally called the "peak power point" (PPP) or "optimal operating point" (OOP) in the literature (Xiao et al. 2006). When the power is plotted against voltage (a P–V plot), the peak power point can be easily recognized, as shown in Figure 1.9.

In most PV power systems, a control algorithm called maximum power point tracking (MPPT) is used to take full advantage of the available solar energy (Xiao et al. 2011). The algorithm is occasionally called "peak power tracking." The term MPPT is used in this book. The real-time operation is to control the PV-side power interface so that the operating characteristics of the load and the PV array always match each other at the MPP. The control objective is to maximize the power output for highest solar energy harvesting at any given instant.

This chapter introduces the MPPT techniques and provides background knowledge about recent developments. Simulations are used to demonstrate the operations that are widely used for practical implementation.

8.1 Background

The principle behind MPPT is the conductance or resistance match between the PV generator output and the load condition, as illustrated in Figure 8.1. In grid-connected systems, the load condition is not as straightforward as in standalone systems, but it can be equivalent to the active power level extracted from the PV generation. The plot shows that the MPP of the PV cell is located at 0.54 V and 8.2 A. When a load rated at 15.2 S in conductance or 66 mΩ in resistance is connected, the maximum power generation is achieved, which is 4.43 W. Any deviation from the ideal load resistance of 66 mΩ, such as an applied load resistance of 0.1 Ω or 0.05 Ω makes the PV cell output deviate from the MPP and produce less power, as illustrated in Figure 8.1.

The majority of loads require either constant voltage or current. When they are directly coupled with the PV generator, the load impedance cannot always be adjusted for the purpose of MPPT. However, when a power interface is connected between the load and PV generator, the load conductance or the impedance at the PV generator terminals can be varied through power conversion. The evolution is demonstrated in Figure 8.2, where a power interface is used between the PV generator and the

Photovoltaic Power System: Modeling, Design, and Control, First Edition. Weidong Xiao.

Companion Website: www.wiley.com/go/xiao/pvpower

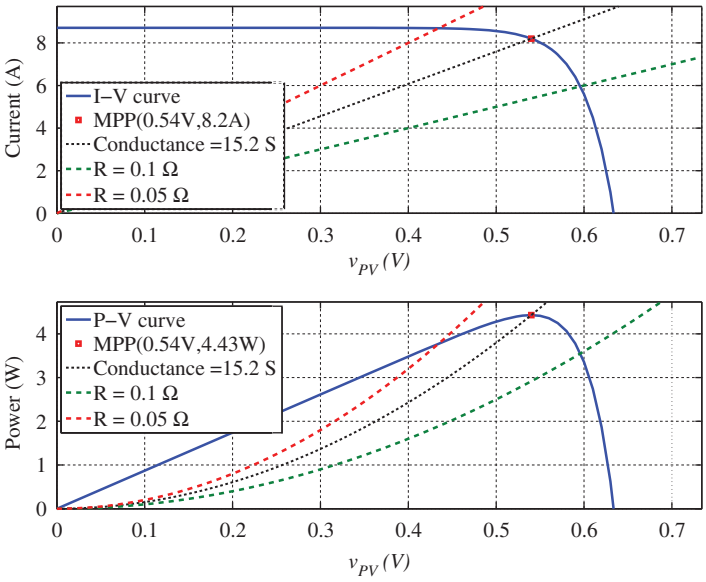

Figure 8.1 Conductance match for maximum power point tracking: top, based on I–V curve; bottom, based on P–V curve.

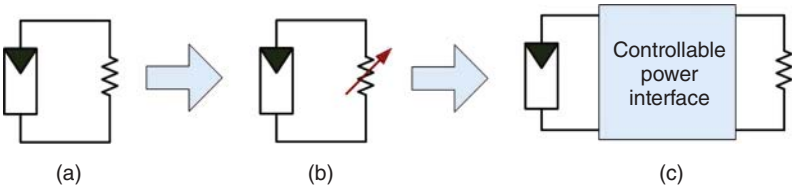

Figure 8.2 Evolution of maximum power point tracking: (a) direct resistor match; (b) variable load match; (c) controllable power interface.

resistive load. The power converter can change the input I–V characteristics from the input to the output and give the equivalent resistance to match the MPP at the PV output terminal. This is the fundamental approach in the latest MPPT technologies.

As discussed in Section 4.1.3, the solar irradiance and cell temperature affect the MPP significantly, as illustrated in Figures 4.8 and 4.9. Dynamic tracking is required to follow unpredictable changes of environmental conditions, particularly the solar irradiance. The cell temperature usually varies with slower dynamics than the irradiance.

The diversity of materials used makes the I–V characteristics different from one PV to another, as illustrated in Figure 1.10. The fill factor (FF) is one way to describe the PV output characteristics; this was introduced in Section 1.6. It is well known that the FF values of crystalline-based PV cells are higher than those of thin-film devices. This fact should be considered to optimally specify the MPPT parameters for different PV output characteristics.

Furthermore, switching-mode power converters are widely used as the power interfaces for PV power generation. As demonstrated in Section 5.1, switching ripples at the PV output terminals make dynamic tracking difficult and reduce tracking efficiency

Table 8.1 Loss analysis of switching-ripple voltage at the PV output terminals.

Percentage voltage ripple (%)	1.0	2.0	5.0	10.0
Percentage power loss (%)	0.03	0.11	0.70	2.99

(Xiao 2007). The power losses caused by ripple voltage in one specific crystalline-based PV module are summarized in Table 8.1. The values can be used as a reference to design the PV-side converter and the control algorithm that will prevent either significant power losses or MPPT malfunctions due to the appearance of voltage ripple. The measurement of voltage and current should be carefully designed since the value difference between the upper and lower peaks in opposite directions can result in significant errors in the measured data.

An MPPT algorithm must generally measure or estimate the PV power output and its variations. For the highest power output, the tracking function is to determine the optimal reference, which can be used as the command or reference to control the power interface. The direct command for switching-mode power converters is either the PWM duty cycle or the phase-shift angle. The reference for the MPPT operation that represents the PV output characteristics can be either the PV-link voltage or current.

The PV-link voltage is considered the most effective reference for MPPT (Xiao et al. 2007b). A feedback loop is required to regulate the PV-link voltage to follow the reference value for the highest power output. An implementation was investigated in Section 7.8 and shown as the block diagrams in Figures 7.1 and 7.2.

It is important to design a proper MPPT algorithm for the power interface in order to achieve the most effective solar energy harvesting. Various techniques have been proposed for the MPPT algorithm (Xiao 2007; Xiao et al. 2011):

- linear approximation
- heuristic search
- extreme value search
- sliding mode
- extremum-seeking control
- real-time identification
- particle swarm optimization (PSO)
- dividing rectangles (DIRECT) algorithm
- intelligent control.

The linear approximation method tries to derive a fixed percentage between the MPP and other measurable signals, such as the open-circuit voltage and short-circuit current. The linear approximation method generally leads to a simple and inexpensive implementation. They are also designed to avoid the problems caused by trial-and-error approaches, commonly referred to as "heuristic search." Some studies have indicated that the optimal operating voltage of a PV module is always very close to a fixed percentage of the open-circuit voltage. MPPT can be achieved by using the open-circuit voltage to predict the optimal operating condition. Similarly, studies have also shown that the optimal operating current can be predicted as a fixed percentage of the short-circuit current. However, the method of linear approximation will not be discussed further

since it has been proven to be inaccurate due to the variation of PV materials and aging and temperature effects (Xiao 2007).

8.2 Heuristic Search

For MPPT, heuristic search is one of the most well-known algorithms thanks to its simplicity and effectiveness. The heuristic search method normally refers to the hill climbing (HC) algorithm, which is an optimization technique. The idea can be simply understood as follows: the top of a hill can be identified if the direction of movement is always up. The algorithm can be used for MPPT since the P–V curve of PV output is hill-shaped. For MPPT, an iteration is applied to change the system operating condition and then sense if the change produces increasing power output (up the hill). If so, the next increment is made in the same direction. In principle, repeating this operation will eventually lead to a maximum, which is the MPP.

The search can also be based on either the P–I curve or the curve of power versus switching duty cycle (P–D), since switching-mode converters are widely used as the PV power interface (Xiao and Dunford 2004b). The switching duty cycle is the control variable used for the majority of PV-side converters, as discussed in Section 5.1. The implementation of the HC algorithm for MPPT is illustrated in Figure 8.3.

The symbol x is the control reference, which can be either the voltage or current of the PV link, or the switching duty cycle if the P–D curve is used for the tracking. The symbol Δx is a constant reflecting the incremental value. The subscripts "new" and "old" are used to represent the recent and historical values of the PV output power and the control variable x. At the end of each MPPT cycle, the latest reference, x_{new}, is output for control.

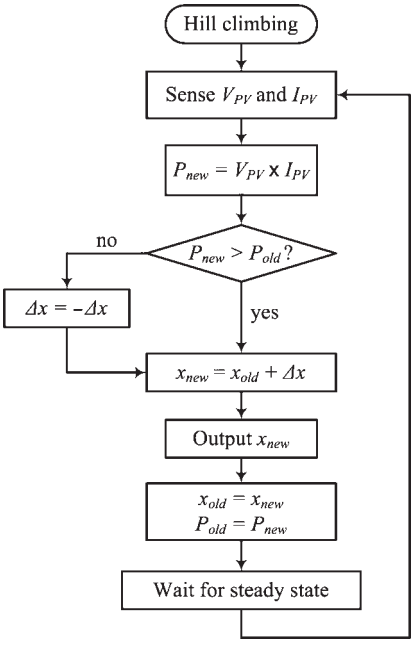

Figure 8.3 Hill climbing algorithm for maximum power point tracking.

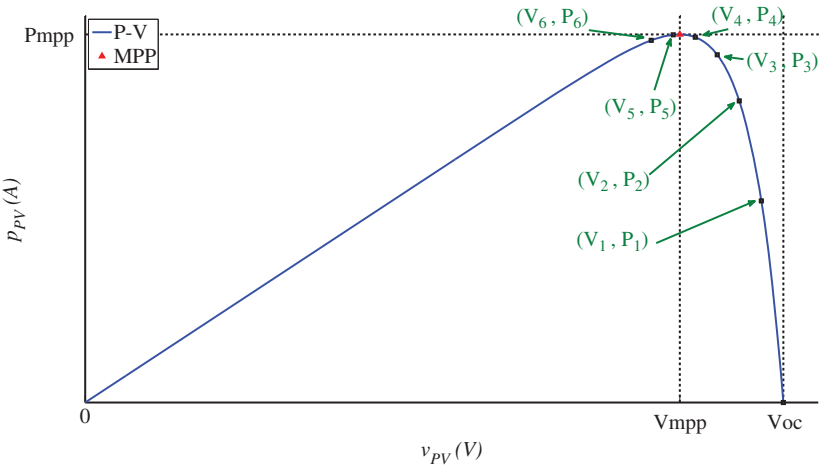

Figure 8.4 Hill climbing based on the P–V curve.

Special attention is given to the "wait for steady state" step at the end of the MPPT loop. When a perturbation is applied, the controller should wait until the system responds and enters a steady state and then make the next measurement. This is important to avoid any misleading information during transient stages, which would cause a malfunction of the MPPT algorithm. The waiting time can be specified in the tracking frequency. The value should be determined according to the system dynamics. The system-dynamics analysis for PV-link voltage regulation was described in Chapters 6 and 7. The tracking time should always be longer than the settling time of the voltage-regulation loop so as to guarantee a stable MPPT operation.

Figure 8.4 illustrates a normalized P–V curve used to demonstrate the HC operation. The initial operation point is commonly referred to the open-circuit condition, V_{oc}, which shows no power output. When the HC algorithm starts, the new operating point (V_1, P_1) is recognized by the MPPT algorithm. The next direction of movement is decided by the corresponding change of power level. Since the new operating point (V_1, P_1) makes the PV modules output more power than the previous one, a relocation to (V_2, P_2) is made by continuing in the same direction. This continues until the movement from (V_5, P_5) to (V_6, P_6), when the MPPT algorithm senses a reduction of the output power by comparing the values of P_5 and P_6. The next direction for the operating point is to move back to (V_5, P_5), and then (V_4, P_4). This process continues until the operating point moves backwards and forwards around the MPP (V_5, P_5). The illustration shows that the HC-based MPPT is capable of finding the local MPP and regulating the system around it.

In the example in Section 5.1.4, the boost topology is used as the PV-side converter (PVSC). At STC, the MPP is the operating condition when the switching duty cycle is 22.9%. The variation of the duty cycle can change the PV power output, as illustrated in Figure 8.5. The hill-shaped P–D curve suits the operation of HC-based MPPT. Following the MPPT procedure, as set out in Figure 8.3, the continuous perturbation of the duty cycle with observation of the power-change direction can identify the MPP, which is at (22.9%, P_{mpp}). The simulation is based on the switching-mode power converter, and

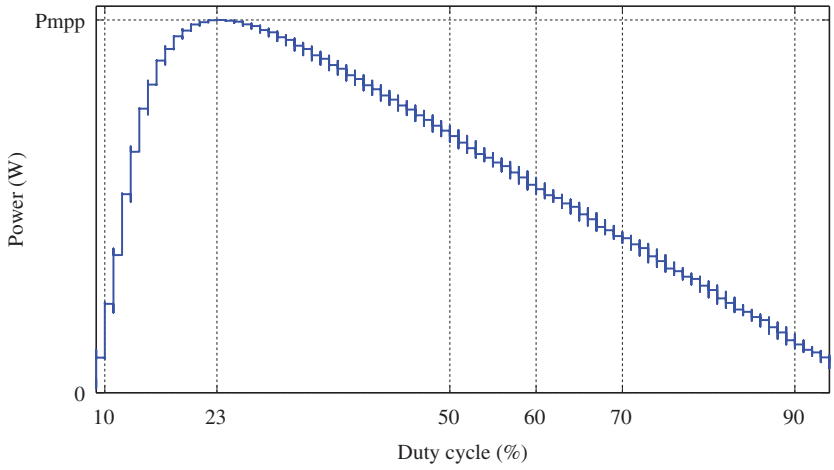

Figure 8.5 Hill climbing based on the P–D curve.

the overshoot and undershoot are noticeable in the recorded curves, caused by the step changes of the duty cycle.

In the steady state, the tracking accuracy of HC-based MPPT is determined by the step size, Δx. The smaller the step size, the higher accuracy in the steady state, since the final oscillation is close to the true MPP, as marked in Figure 8.4. On the contrary, a high value of Δx indicates a fast tracking process, since fewer steps are required to reach the area near the MPP. Continuous perturbation and observation is generally a robust and effective way to locate the MPP in real-time, regardless of any variations of solar irradiance and cell temperature.

HC-based MPPT is commonly referred to as the method of perturbation and observation (P&O), and it is frequently discussed in the MPPT literature. It should be noted that the principle of P&O is the same as the HC algorithm; P&O is simply a dedicated term used for the MPPT algorithm in PV power systems. The HC algorithm is a generic optimal algorithm, with uses in fields other than MPPT. A perturbation is always required to run heuristic search algorithms, such as HC or P&O. The two terms are equivalent. In the following sections, only HC-based MPPT is referred to, so as to avoid confusion.

A Simulink model can be built to simulate HC-based MPPT, as shown in Figure 8.6. It can be implemented by following the flowchart in Figure 8.3. The latest measured power level *Pnew* is compared with the previous measurement *Pold* to determine the sign of the next perturbation. The perturbation amplitude is implemented in the unit delay block, indicated by *delta-x*. The sign of *delta-x* is always determined by the comparison between *Pnew* and *Pold*. The MPPT output is shown as *Xnew* and can be either increased or decreased from the previous value, *Xold*. The tracking frequency is implemented in the three unit delay blocks using the settling of the sample time. Special attention is given that the sampling time of the unit delay blocks matches the MPPT tracking speed, which is specified by the system dynamic analysis. The sampling time for MPPT should not be confused with the sampling time for the overall system simulation.

Continuous oscillation around the MPP is an intrinsic problem of the standard HC-based MPPT algorithm (Xiao and Dunford 2004b). If the incremental step is low, it takes a long time to find the MPP initially or after a change in environmental conditions.

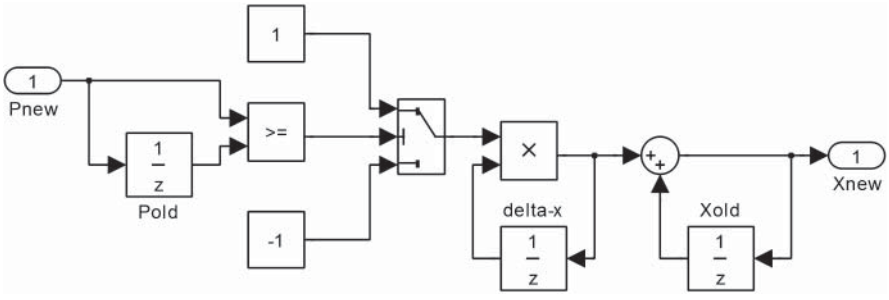

Figure 8.6 Simulink model of the hill-climbing-based maximum power point tracking.

However, if a high value of Δx is used, the power fluctuation is significant around the MPP and results in energy waste, as detailed in Table 8.1. The tradeoff between tracking accuracy and speed should always be considered when a fixed value of Δx is used for HC-based MPPT.

8.3 Extreme-value Searching

One development of MPPT is based on the extreme value theorem (EVT), according to which the extremum, either maximum or minimum, occurs at a critical point, as expressed in (8.1). The critical point x_0 is the local extremum found from $y(x_0)$, where y is a function of x. The critical point can be continuously tracked and updated to follow (8.1).

$$\left.\frac{dy(x)}{dx}\right|_{x=x_0} = 0 \tag{8.1}$$

For the PV output, the power reaches a local peak if the condition is satisfied by (8.2), which assumes that p_{pv} is a function of v_{pv}. Based on the EVT, an MPPT algorithm can be developed.

$$\left.\frac{dp_{pv}(v_{pv})}{dv_{pv}}\right|_{v_{pv}=V_{mpp}} = 0 \tag{8.2}$$

As discussed in Chapter 4, the function p_{pv} with respect to v_{pv} can be established. However, the coefficients of the function are constant only when the environmental conditions in terms of solar irradiance and cell temperature are steady. In the real world, the function is time-variant due to environment variations. Furthermore, the mathematical model coefficients of the PV cell are difficult to identify in real time.

One approach uses a numerical approach – the Euler method – to approximate the operation of the extreme value search. The approximation approach does not require a mathematical model to represent the PV output characteristics. The truncation error should be considered in the numeral differentiation, as pointed out by Xiao et al. (2007a). Therefore, the numerical differentiation can be expressed by (8.3) and (8.4), which are based on the forward Euler and backward Euler methods, respectively.

$$\left.\frac{dp_{pv}}{dv_{pv}}\right|_{V_{k-1}} = \frac{P_k - P_{k-1}}{\Delta V_k} + O(\Delta V^2) \tag{8.3}$$

where $\Delta V_k = V_k - V_{k-1}$.

$$\left.\frac{dp_{pv}}{dv_{pv}}\right|_{V_k} = \frac{P_k - P_{k-1}}{\Delta V_k} + O(\Delta V^2) \tag{8.4}$$

The expressions are represented in discrete time, where P_k and P_{k-1} are the adjacent records of the measured power, and V_k and V_{k-1} are sequential values of the measured voltage. The local truncation error for the Euler methods is equal to $O(\Delta V^2)$, which stands for the order of ΔV. The expressions in both (8.3) and (8.4) indicate first-order accuracy (Xiao et al. 2007a). The local truncation error is defined to represent how well the exact solution satisfies the numerical scheme. The capital O notation is used to characterize the residual term of a truncated infinite series in mathematics. According to (8.3) and (8.4), the MPP is considered to be tracked if the condition of (8.5) is satisfied when the value of the truncation error is insignificant and $P_k \approx P_{k-1}$.

$$\frac{P_k - P_{k-1}}{\Delta V_k} + O(\Delta V^2) = 0 \tag{8.5}$$

Another MPPT algorithm that is frequently discussed in literature, and which is based on the EVT, is the incremental conductance method (IncCond). Its mathematical expression is

$$\frac{dp_{pv}}{dv_{pv}} = \frac{d(v_{pv})i_{pv}}{dv_{pv}} = i_{pv} + v_{pv}\frac{di_{pv}}{dv_{pv}} = 0 \tag{8.6}$$

where the differentiation is changed from dp/dv to di/dv since $p = v \times i$. The numerical approximation based on the Euler method is

$$I_k + V_k\frac{(I_k - I_{k-1})}{\Delta V} + O(\Delta V^2) = I_k + V_k\frac{\Delta I_k}{\Delta V_k} + O(\Delta V^2) \approx 0 \tag{8.7}$$

The IncCond method is established according to the equilibrium and is expressed as

$$-\frac{I_k}{V_k} \approx \frac{\Delta I_k}{\Delta V_k} \tag{8.8}$$

The flowchart of the IncCond algorithm is illustrated in Figure 8.7. When the condition

$$-\frac{I_k}{V_k} < \frac{\Delta I_k}{\Delta V_k} \tag{8.9}$$

is met, the current operating point is expected to be on the left-hand side of the MPP in the I–V curve. An increase of v_{pv} should be executed in order to approach the MPP. This is equivalent to the condition, $dp/dv > 0$. On the other hand, the algorithm sends a command to decrease v_{pv} when the equivalent condition, $dp/dv < 0$ is detected. The perturbation that is caused by the reference change can be stopped if the equilibrium in (8.8) is satisfied according to the IncCond algorithm. This indicates that the MPP has been successfully located and that the perturbation should be stopped. This aims to eliminate a steady-state oscillation around the MPP, which is an intrinsic problem of using the HC-based MPPT algorithm.

However, there are still oscillations under stable environmental conditions when the IncCond algorithm is applied. The condition in (8.2) is seldom satisfied in practical

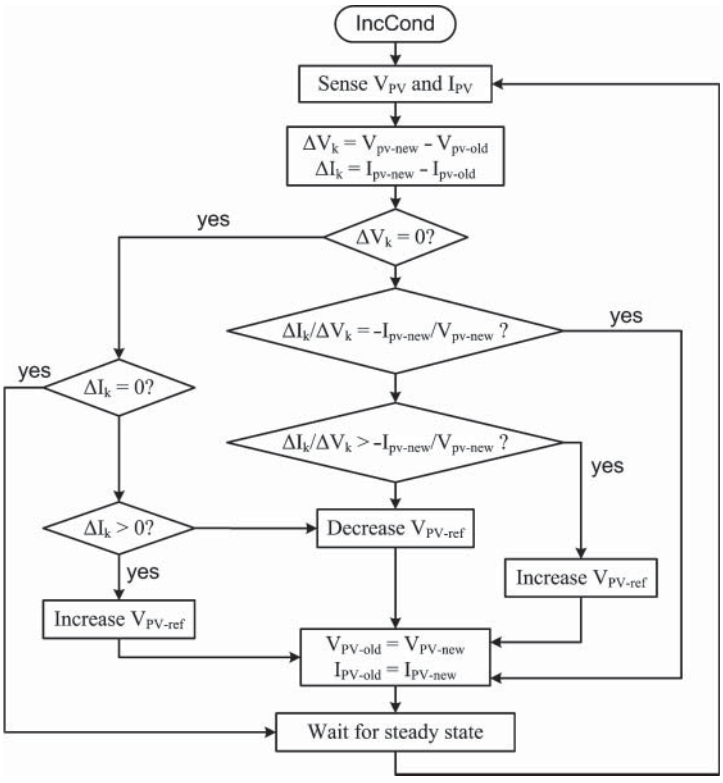

Figure 8.7 Flowchart for extreme value searching.

PV systems. The numerical approximation of the maximum power condition rarely matches the true MPP, which is represented in the continuous time by $dp_{pv}/dv_{pv} = 0$.

This issue, as explained by Xiao et al. (2007a), is caused by the numerical approximation. According to (8.3) and (8.4), the local truncation error of a numerical derivation is always present in Euler methods. Section 8.8 will introduce one approach for reducing the truncation error in order to improve the EVT-based MPPT algorithm.

8.4 Sampling Frequency and Perturbation Size

It should be noted that the MPPT implementation for both HC and EVT is based on digital control in discrete time. The flowcharts of the HC and IncCond, as shown in Figures 8.3 and 8.7, respectively, always update the control reference and indicate the waiting time for the system entering the next steady state. Therefore, one important parameter to execute the MPPT is the perturbation frequency, which is denoted as f_{mppt}. When the dynamic model is derived at the PV link, the value of f_{mppt} can be determined from the settling time of each step response. For example, if the P–D curve is used for the tracking, the dynamic model developed in Section 5.1 should be used to evaluate the settling time. If the P–V curve is applied, the system dynamics is considered using the voltage regulation loop, as described in Sections 6.3 and 7.8.

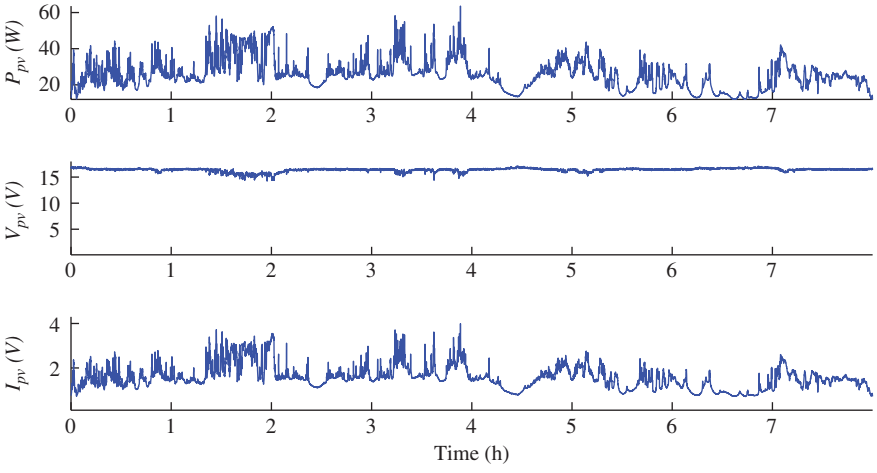

Figure 8.8 Waveforms of PV power (P_{pv}), voltage (V_{pv}), and current (I_{pv}) measured on 9 July 2006.

The perturbation size should be determined with consideration of the ripples that are caused by the switching-mode power interface. For practical applications, the signal-to-noise ratio (SNR) should be considered to avoid any misleading information for the MPPT operation. The noise and ripples in the measured signal can cause malfunctions of MPPT algorithms. The tradeoff of the tracking speed in transient states and the accuracy in steady states should also be considered.

Determining the optimal step size becomes even more difficult if weather variation patterns are considered. Figure 8.8 shows the waveform of the measured power, voltage, and current of a specific circumstance. The eight-hour test was performed in Vancouver, Canada. It is noticeable that the PV power level varies dramatically over a daily period and causes significantly fast dynamics for the MPPT algorithm. For the best energy harvesting under any specific weather conditions, the dynamic performance of MPPT should be emphasized more than the steady state. Large perturbations are expected, which allows for fast tracking of changes of the MPP.

Based on the same PV power system, Figure 8.9 shows a different example, which is a good sunny day. The PV generating power increases smoothly in the morning and decreases slowly in the afternoon. The environmental conditions become predictable. This is commonly considered as an ideal condition for energy harvesting, and the MPPT algorithm shows good performance in the steady state. Some dry areas, such as the Arabian Gulf countries, show similar patterns year round. Comparing the case studies shown in Figure 8.8 and 8.9, a single optimal value of the perturbation size is difficult to choose due to the tradeoff of the tracking speed and accuracy and the regional differences (Du et al. 2015).

8.5 Case Study

The buck converter used for the PV-side power interface was designed in Section 5.1.2, dynamically modeled in Section 6.3.2, and its control was described in Section 7.8.3. This example is based on the same system parameters, and will reveal the approaches

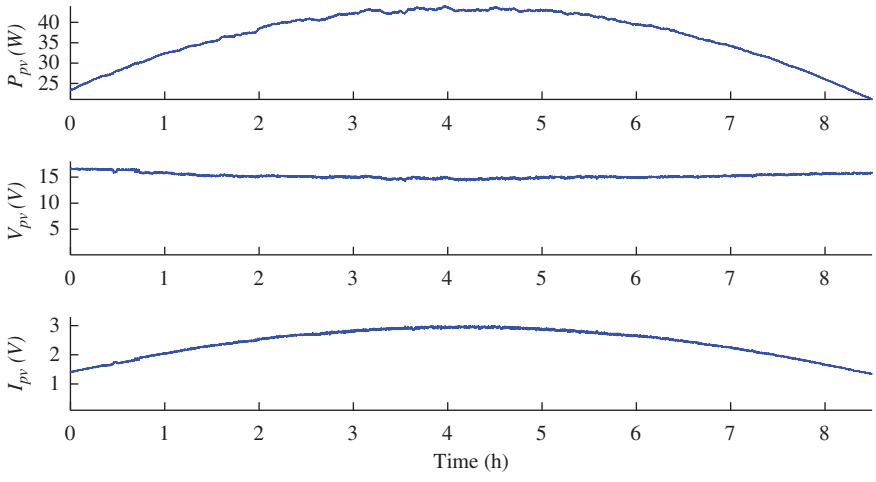

Figure 8.9 Waveforms of PV power (P_{pv}), voltage (V_{pv}), and current (I_{pv}) measured on 24 June 2006.

Table 8.2 Dynamic analysis of the buck converter used for the PV-side power interface.

Configuration	Overshoot	Settling	Description in	Illustration
Original plant for P–D MPPT	69%	9.6 ms	Section 6.3.2	Figure 6.4
Closed-loop for P–V MPPT	≈ 0	1.7 ms	Section 7.8.3	Figure 7.15

to system design, modeling, and control. According to the control diagram, as shown in Figure 7.1, an MPPT block needs to be implemented. Therefore, the system dynamics should be analyzed before the design of the MPPT. The important information about the original dynamics and the closed-loop performance are summarized in Table 8.2. For this case study, the MPPT operation is based on the HC algorithm.

Without the voltage regulation loop, HC-based MPPT can be operated with the P–D curve, which shows the MPP with respect to the switching duty cycle. The minimal perturbation time can be determined from the settling time, which is estimated as 9.6 ms. When the voltage regulation loop is implemented, the system response is improved, with a settling time of 1.7 ms. The minimal perturbation time, which is the response of P_{pv} to a change of v_{pv}, can be selected from the settling time. With a voltage regulation loop, HC-based MPPT can operate five times faster than without.

Figure 8.10 illustrates the overall simulation model, including the blocks for the PV array and DC/DC buck converter. The control functions are the PWM signal generator, the MPPT function, and the PID controller for PV-link voltage regulation. The MPPT algorithm evaluates the power variation and decides the reference for the PV-link voltage. The voltage regulation loop follows commands in order to stay at the MPP regardless of variations of irradiance and temperature.

The MPPT sampling frequency is 400 Hz according to the settling time when the voltage regulation loop is implemented. The simulation sampling frequency 50 MHz, of which one thousand samples are filled for each switching cycle. It should not be confused by the MPPT sampling frequency.

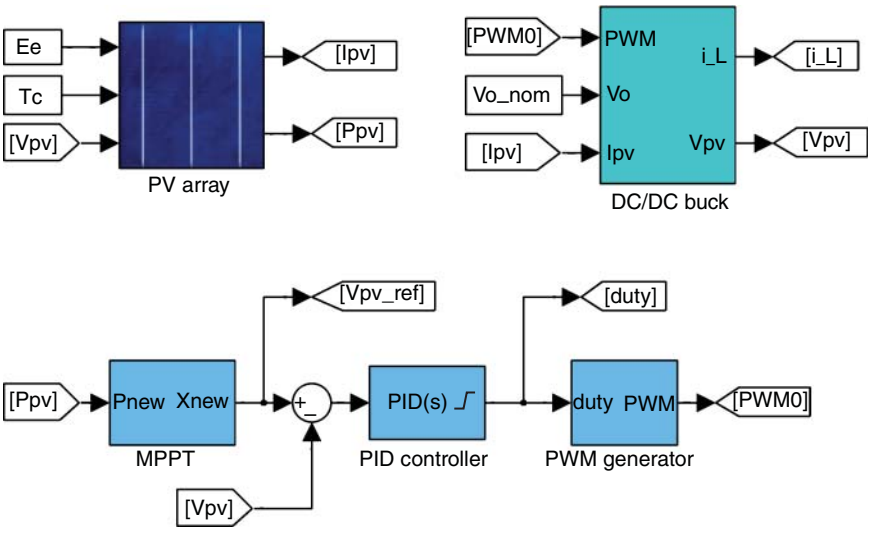

Figure 8.10 Simulink model of the buck converter used for PV-side power interface with MPPT.

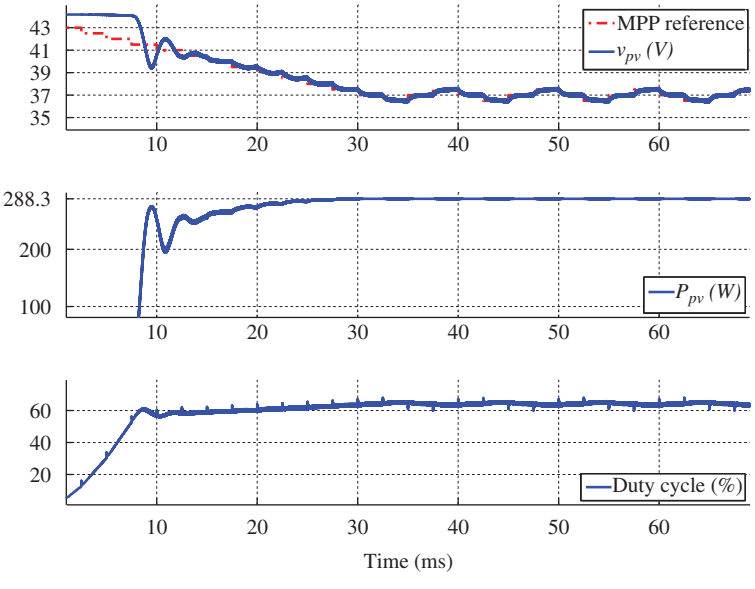

Figure 8.11 Simulation result of the buck converter used for PV-side power interface with MPPT.

The simulation result is shown in Figure 8.11, and includes the MPPT reference signal that is generated by the MPPT algorithm. The voltage regulation loop follows the commands to reach the MPP. After the transient stage, about 34 ms, the HC-based MPPT algorithm continues the perturbation process and maintains the operating point around the MPP. The peak power is 288.3 W. This is shown in the power waveform and agrees with the PV module specification, as shown in Figure 5.4. The switching duty cycle is the direct control variable for the DC/DC buck converter, and is also shown in Figure 8.11.

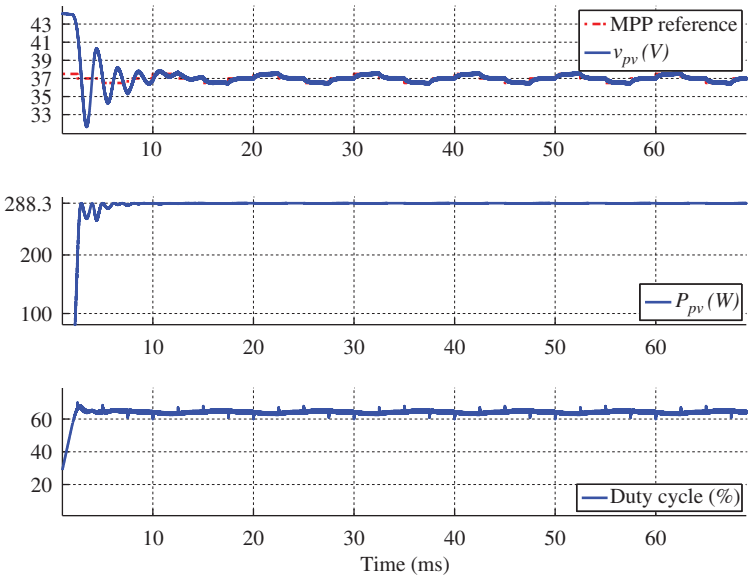

Figure 8.12 Simulation result of the buck converter used for PV-side power interface with MPPT.

The case study demonstrates the HC-based MPPT function and shows the effectiveness of the proposed design, modeling, control, and simulation approaches.

For the regulation for the PV output voltage, the initial position of the MPP can be estimated from the open-circuit voltage, as discussed at the beginning of Chapter 7. In this case, the initial value can be set to be 38 V, which is equivalent to 85% of the open-circuit voltage. The simulation result with the implementation of the initial value is illustrated in Figure 8.12. This shows the steady state is reached for the MPP at 16 ms, in contrast to the 34 ms in Figure 8.11. This shows that an effective way to avoid long tracking times at the initial stage and demonstrates the advantage of using the voltage control loop. The PV-link voltage is an useful reference for MPPT and other purposes, since it does not vary significantly with the irradiance.

8.6 Start-stop Mechanism for HC-based MPPT

One drawback of HC-based MPPT is the intrinsic oscillation at the steady state, which causes energy waste. Even though the incremental conductance method is based on the extremum search theorem, it cannot completely stop oscillations in the steady state due to the truncated error of the numerical differentiation, as described in Section 8.3. One proposed solution is the start-stop mechanism (Khan and Xiao 2016). A three-point oscillation pattern can be identified in the steady state when the MPP is found, as shown in Figures 8.11 and 8.12. A detailed view of three-point oscillation is given in Figure 8.13. This includes the waveform of v_{pv} in a time series together with the P–V curve. The HC-based algorithm directs the operating point alternately to the three points, a, b, and c, which causes the steady oscillation.

The simple idea proposed is to stop the active tracking when the three-point oscillation pattern is identified. Two operation modes are defined: one is called

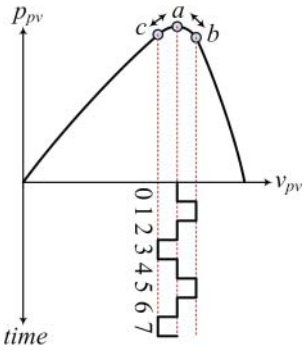

Figure 8.13 Three-point oscillation caused by HC-based MPPT.

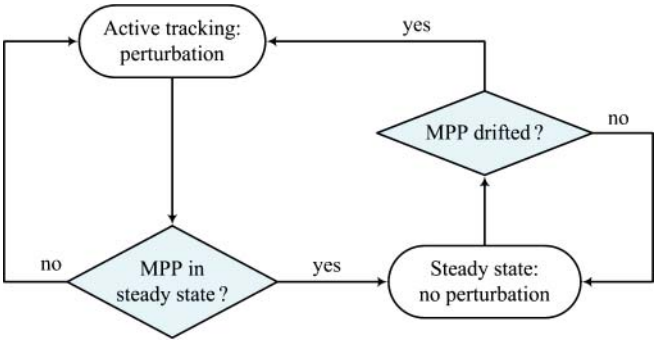

Figure 8.14 Flowchart of the start-stop mechanism for hill-climbing operation.

"active tracking" and the other is the "steady state," as shown in Figure 8.14. The HC algorithm represents the active tracking mode, comparing the power variation and the perturbation direction. The steady-state operating mode stops the perturbation and maintains a constant reference for system regulation. PV-link voltage regulation is commonly used to maintain the steady state. The system status is continuously evaluated to detect if the MPP has changed, something that is commonly caused by a variation of environmental conditions. When this is confirmed, active tracking is reactivated until a new steady-state MPP is identified.

The oscillation pattern can be recognized when the perturbation is around the MPP. The perturbation direction changes every two cycles. This phenomenon can be expressed as

$$\Delta V_k = -\Delta V_{k-2} \tag{8.10}$$

where the perturbation step of the HC algorithm is defined as ΔV_k, where the k shows the data sequence in discrete time.

Figure 8.13 illustrates that the step sign is positive at the moment 1, but it is negative at moment 3. The sign is negative at moment 3, but it becomes positive at moment 5. The condition holds true repeatedly in the steady state and shows the three-point oscillation pattern. Therefore, the steady state around the MPP can be identified when three of four consecutive sampling cycles satisfy the condition of (8.10). For robust operation in a practical implementation, it is recommended to look at more than ten cycles before a stop decision is made.

When the perturbation is stopped, the system is controlled in the steady-state mode since the MPP has been found. The PV voltage is regulated to a constant value, which represents the MPP. The output power is continuously sensed and monitored during the steady-state operation. When the power level detected is different from the reference value, the MPP is considered to have drifted to a new value due to environmental variation. The active tracking via the HC algorithm should be activated again to find the new MPP. The start-stop mechanism formed in this way avoids the oscillation problem typical of the HC-based MPPT method.

To evaluate the effectiveness of the start-stop mechanism, a simulation based on the case discussed in Section 8.5 is conducted. A Simulink model is built to combine the start-stop mechanism with HC-based MPPT, as shown in Figure 8.15. Based on the measured power from the PV output, P&O can be conducted and compared with the historical value. The active tracking is implemented in the perturbation block, which is the standard format of the HC algorithm.

The start-stop mechanism estimates the condition and decides to pass the perturbation or stop it. When the steady state is detected, the perturbation signal is assigned to zero in order to stop the perturbation. Otherwise, it follows the output of the perturbation block. The signal shown as Xnew is the control output from the MPPT block, which is updated from the historic value, Xold. The signal represents the PV output voltage reference for the voltage feedback loop when the P–V curve is used for MPPT. The signal can also be the direct control signal, the switching duty cycle for the power interface, when the P–D curve, as illustrated in Figure 8.5, is applied for MPPT.

Figure 8.16 illustrates the Simulink implementation of the start-stop mechanism. Its inputs are the perturbation signal from the perturbation block and the latest power measurement. The status symbol "mode," commands active tracking if the value is 1. A value of 0 leads to the stop mode, which sets the signal Delta-x to zero. The three-point pattern is detected by evaluating (8.10). When the three-point pattern is clearly recognized over a number of cycles, the stop mode commences and the value of PV output power is recorded as the benchmark. The cycle limit is implemented inside the relay block; it is assigned a value of 11 in this case study.

When the system enters the stop mode, the benchmark value is continuously compared with the new measurement of the PV output power. When the difference becomes significant, the mechanism is reset to pass the perturbation and perform active HC tracking. In this case study, the threshold is assigned a value of 3 W. In general, the start-stop mechanism performs the function of evaluation and decision as illustrated in Figures 8.14 and 8.15.

The simulation results are illustrated in Figure 8.17, which includes the waveforms of v_{pv}, p_{pv}, and the switching duty cycle. When the three-point condition, as expressed

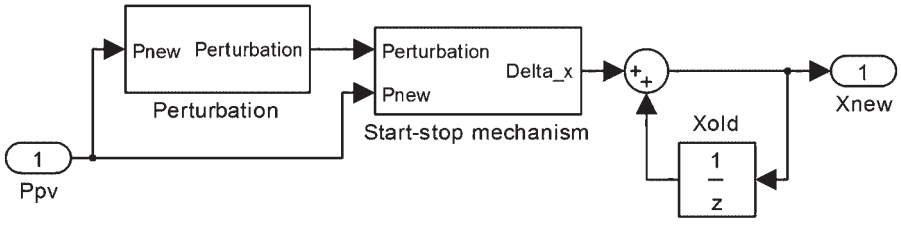

Figure 8.15 Simulink model for integration of start-stop mechanism with HC-based MPPT.

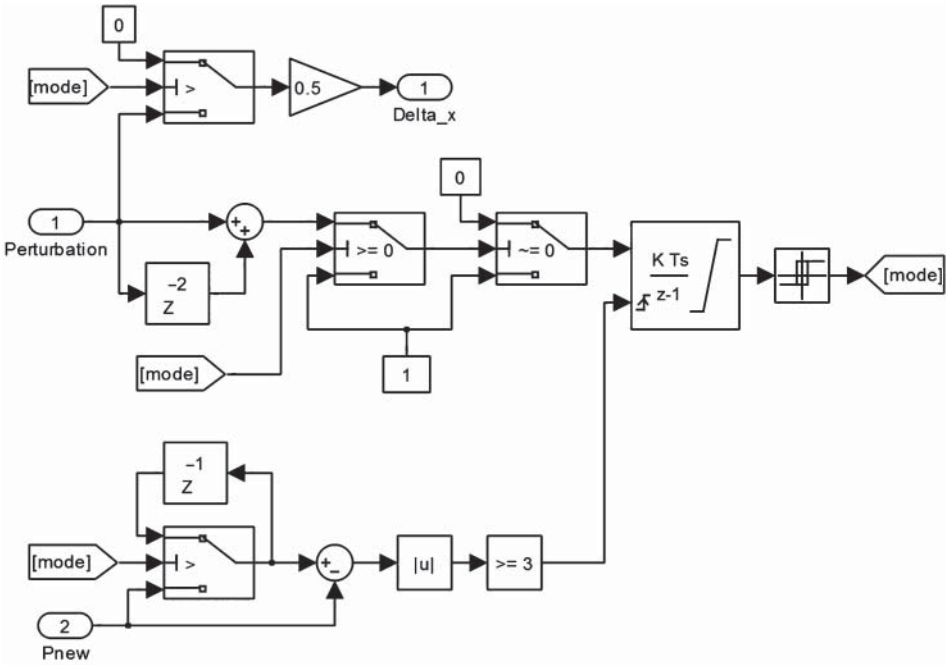

Figure 8.16 Simulink model of the start-stop mechanism.

in (8.10), is satisfied for 11 cycles consecutively, the perturbation is stopped from the MPPT block output, as shown at 33 ms. The voltage of the MPP is determined to be 37 V and is kept steady. A step change of the irradiance from 1000 $\mathrm{W/m^2}$ to 500 $\mathrm{W/m^2}$ is applied at 60 ms. The power variation triggers the active tracking mode to restart, the assumption being that the MPP has drifted to a new value. The active tracking locates the new MPP. After the condition of (8.10) is satisfied over 11 cycles, the perturbation operation is stopped again at 93 ms. The voltage of the new MPP is determined to be 36 V and is the system is then kept steady in this state. The start-stop mechanism has been proven to be a simple and effective way to avoid oscillations in the steady state and to improve the MPPT performance (Khan and Xiao 2016). The effectiveness and improvement can be demonstrated by comparing the simulation results in Figures 8.12 and 8.17.

8.7 Adaptive Step Size Based on the Steepest Descent

Another idea has been proposed to target the drawbacks of HC-based algorithms. This is called the adaptive HC method, and involves dynamic adjustment of the perturbation size (Xiao and Dunford 2004b). When there is an oscillation pattern during MPPT, it is ideal to make the perturbation size significant during the transient stage, but to assign it a low value when the steady state is reached for the MPP.

An optimization method can again be used to achieve the target. One algorithm is the steepest descent method, which is designed to find the nearest local minimum. The same principle can be applied to find the local maximum value – the MPP – when the gradient